Research Article

CFAR Detection from Noncoherent Radar Echoes Using Bayesian Theory

Hiroyuki Yamaguchi and Wataru Suganuma

Air Systems Research Center, Technical R & D Institute, Ministry of Defense, 1-2-10 Sakae, Tachikawa, Tokyo 190-8533, Japan

Correspondence should be addressed to Hiroyuki Yamaguchi, yama@ieee.org

We propose a new constant false alarm rate (CFAR) detection method from noncoherent radar echoes, considering heterogeneous sea clutter. It applies the Bayesian theory for adaptive estimation of the local clutter statistical distribution in the cell under test. The detection technique can be readily implemented in existing noncoherent marine radar systems, which makes it particularly attractive for economical CFAR detection systems. Monte Carlo simulations were used to investigate the detection performance and demonstrated that the proposed technique provides a higher probability of detection than conventional techniques, such as cell averaging CFAR (CA-CFAR), especially with a small number of reference cells.

1. Introduction

Noncoherent radar systems are widely used in applications such as ship navigation, and radar signal detection from sea clutter has been the subject of intense research for a number of years. Considerable experimental and theoretical investigations have studied the feasibility of detection with a constant false alarm rate (CFAR). In CFAR detection, the local sea clutter power in a range cell under test (CUT) is adaptively estimated from samples adjacent to the CUT, which are referred to as reference cells. The estimation method is very important for detection probability enhancement, and many studies have been reported.

For example, if the radar illuminates a large sea area, then the probability distribution of the envelope of sea clutter is approximated by a Rayleigh distribution [1]. Thus, the sea clutter in a noncoherent radar system with a square law detector is exponentially distributed. In this sea clutter, the local mean clutter power is spatially a constant (i.e., homogeneous clutter). The local clutter power can then be estimated by the maximum likelihood (ML) method. CFAR implemented using ML is known as cell averaging CFAR (CA-CFAR) [2, 3]. If the clutter power varies spatially (i.e., heterogeneous clutter), however, a K distribution provides a good phenomenological expression of the sea clutter,

especially for high-resolution radar at low-grazing angle [4–9]. Using CFAR detection against K distributed clutter, the maximum a posterior (MAP) or the minimum mean square error (MMSE), that is, Bayes risk minimization method, can be applied for the clutter power estimation [10, 11]. By implementing these estimation methods, the spatial correlation of the clutter power is regarded as strong. Thus, the assumption can be made that the local clutter power in the CUT equals that in the reference cells.

However, results of the measured sea clutter in [8, 9, 12] indicate that the spatial correlation of the clutter power is about a few tens of meters. If the reference cell extent, which is obtained by multiplying the range cell scale by the number of reference cells, is more than the spatial correlation length of the clutter power, the above assumption cannot be accepted. Thus, a mismatch can occur between estimated and actual clutter power. This mismatch affects the detection performance, that is, the probability of detection degradation. In addition, the estimation accuracy does not increase with the number of reference cells. One way to overcome this problem lies in enhancing the probability of detection by using a small number of reference cells, because the local clutter power can then be regarded as almost constant. In addition, CFAR detection with a small number of the cells can provide distributed target detection, for

example, identify closely separated ships or a ship near land, compared with conventional CFAR using a large number of cells [13].

In this study, a CFAR detection technique is introduced for heterogeneous sea clutter with a noncoherent radar system, where the local clutter power in the CUT is estimated by the Bayesian theory. Typically, this requires sufficient prior information about the sea clutter to be incorporated in the estimation, or the estimation accuracy might be degraded, as with ML and MAP. In the proposed technique, however, CFAR detection is achieved without this prior information. A Bayesian optimum radar detector (BORD) has been reported [14] as one application of CFAR to Bayesian theory. However, the BORD is a coherent radar system and is difficult to implement with a noncoherent system, since complex data, such as the Doppler frequency, is not available. To investigate the detection probability of the proposed technique, Monte Carlo simulations are performed under various sea clutter conditions, including consideration of the spatial correlation of the clutter power. The results are also compared with conventional CFAR techniques, such as CA-CFAR, and show the usefulness of the proposed technique, especially for a small number of reference cells. In the proposed technique, data from the square law detector is processed, allowing easy implementation in existing noncoherent radar systems, such as marine radar, making it particularly attractive for an economical CFAR detection system. In addition, the proposed technique can be applied to high resolution radar, with a range resolution of 4 m [5, 8], since heterogeneous clutter is supposed.

In the next section, the clutter and the target signal model are described and then the proposed detection technique. In Section 3, the detection performance with various clutters is investigated. Finally, Section 4 concludes this study.

2. Detection Technique

The detection problem of interest here is that if we suppose a noncoherent radar to transmit a pulse and receive the radar echo. The echo is then detected via a square law detector and sampled by an A/D converter. Here, the sampled echo in the CUT and the echoes from M reference cells are denoted as X and $D = \{X_1, \ldots, X_M\}$, respectively, as shown in Figure 1. Note that cell size adaptation with respect to the target size is outside the scope of this study. When the target signal is absent from the CUT, it is assumed that X consists of only the clutter; when the signal is present, it is assumed that X consists of the sum of the clutter and the target signal and is statistically independent of the clutter. Additionally, the system noise is sufficiently small compared with the clutter and is neglected. Note that information about the sea clutter is not available, since the sea clutter's statistical characteristics might change frequently with factors such as the wave structure.

2.1. Sea Clutter and the Target Signal Model. Assume that the sea clutter is heterogeneous and modeled as the compound Gaussian, as described in [6, 7, 10, 15]. From these references,

the clutter C can be represented by the product of two independent random variables

$$C = \tau x, \tag{1}$$

where x and τ are named speckle and texture, respectively. The variable x is given by a noncorrelated exponential random variable. The variable τ represents the local clutter power, that is, the mean of the underlying conditional exponential distribution.

In general, local clutter power fluctuations are induced by spatial and temporal variations in the clutter. Their correlation lengths are a few tens of meters and the order of seconds, respectively [9, 16]. Because its long temporal correlation time, local clutter power is regarded as a constant during CFAR processing intervals. Thus, modeling the spatial power distribution is important in CFAR detection. In [7], for example, the distribution function of the power is given by a Gamma distribution, that is, the distribution function of the clutter is the K distribution, which is a function of the scale and shape parameters. In this study, the distribution function of the power is given by an inverse Gamma distribution because this is a conjugate prior distribution [17]. By using this prior, a prior and posterior distributions belong to the same class of distributions. Thus, transition from prior to posterior only involves a change in the parameters with no additional calculation, which reduces the computational complexity. We must consider the justification of the inverse Gamma distribution. In the performance analysis in Section 3, the local clutter power of the simulated sea clutter is given as Gamma distributed (not inverse Gamma). To determine the validity of the proposed technique applying the inverse Gamma prior, analysis is performed using simulated sea clutter. The inverse Gamma distribution is also a function of the shape and scale parameters (these parameters differ from those in the Gamma distribution). However, no information about the clutter is available, so the parameters are not known a priori.

Generally, atmospheric propagation effects (i.e., clear sky, rain, etc.), target scintillation, and so on, cause the target signal to fluctuate. From a radar specification point of view, the pulse repetition frequency (PRF) is a few kHz, since marine radar is assumed in this study. Thus, target scintillation might be neglected during CFAR processing intervals; the target echo fluctuates slowly relative to the order of magnitude of the PRF. Therefore, the target model is assumed as Swerling I, which has been largely used in radar literature [18]. In this model, signal fluctuation is given by an exponential distribution and the mean of the fluctuation represents the signal power.

2.2. Proposed Technique. Similar to CA-CFAR, the test statistic T in the proposed technique is defined as

$$T = \frac{X}{\hat{\tau}}, \tag{2}$$

where $\hat{\tau}$ is the estimated local clutter power in the CUT, based on the Bayesian theory. Signal detection is made by
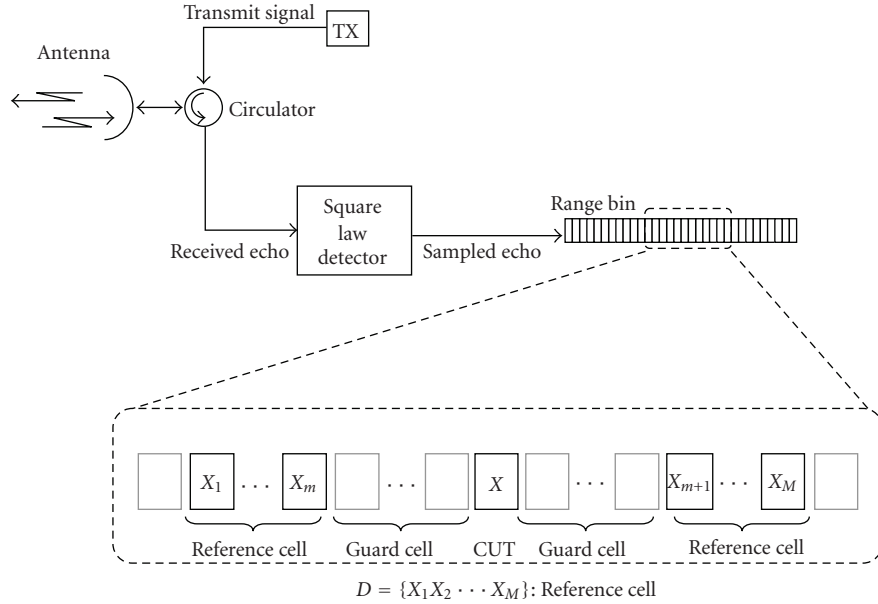
FIGURE 1: Data in CUT and reference cell.

comparing T with a threshold level η; if $T \geqq \eta$ (or $T < \eta$), the target signal is present (or absent). The threshold is given from the false alarm rate. In addition, the clutter in the CUT and the power are estimated by the Bayesian. With these estimated values, the proposed CFAR detection is formulated. The following explains the estimated values by the Bayesian theory and provides the false alarm rate and the probability of detection.

2.2.1. Local Clutter Power Estimation. Suppose that both X and D contain no target signal, and that the local clutter power in the CUT is the same as that in the reference cells. Based on Bayesian theory, a posterior distribution of the local clutter power in the CUT τ conditioned on X and D is expressed as

$$p(\tau \mid X, D) = \frac{L(\tau \mid X, D)p(\tau)}{\int_0^\infty L(\tau \mid X, D)p(\tau)d\tau}, \quad (3)$$

where $L(\tau \mid X, D)$ and $p(\tau)$ are a likelihood function and a prior distribution of the local clutter power τ. The likelihood function is given by

$$L(\tau \mid X, D) = p(X \mid \tau) \times \prod_{m=1}^{M} p(X_m \mid \tau), \quad (4)$$

where $p(X \mid \tau)$ and $p(X_m \mid \tau)$ are an exponential distribution conditioned on τ

$$p(X \mid \tau) = \frac{1}{\tau}e^{-X/\tau}, \qquad p(X_m \mid \tau) = \frac{1}{\tau}e^{-X_m/\tau}. \quad (5)$$

The prior distribution, that is, the assumed local clutter power distribution, is the inverse Gamma distribution, as mentioned in Section 2.1. This is denoted by $IG(\tau; \alpha_0, \beta_0)$,

with α_0 of the shape parameter and β_0 of the scale parameter, that is, hyperparameters. Thus,

$$p(\tau) = IG(\tau; \alpha_0, \beta_0) = \frac{\beta_0^{\alpha_0}}{\Gamma(\alpha_0)}\tau^{-\alpha_0-1}e^{-\beta_0/\tau}. \quad (6)$$

Since the inverse Gamma distribution is the conjugate prior, the posterior distribution $p(\tau \mid X, D)$ in (3) is also the inverse Gamma. Thus, $p(\tau \mid X, D) = IG(\tau; \alpha_1, \beta_1)$. The hyperparameters are represented by

$$\alpha_1 = M + 1 + \alpha_0, \quad (7)$$

$$\beta_1 = \sum_{m=1}^{M} X_m + X + \beta_0. \quad (8)$$

Therefore, the distribution of the estimated local clutter power $\hat{\tau}$ based on the Bayesian theory is given by

$$p(\hat{\tau} \mid X, D) = IG(\hat{\tau}; \alpha_1, \beta_1). \quad (9)$$

Next, we have to consider the value of $\hat{\tau}$ to output T in (2). As seen in (9), $\hat{\tau}$ is not estimated as the point value but as the distribution. Thus, we propose that the estimated local clutter power is given as a random variable whose distribution is the inverse Gamma, that is, $\hat{\tau} \sim IG(\hat{\tau}; \alpha_1, \beta_1)$ ("$\sim$" means "distributed as"). By using a Gaussian random number generator, the estimated local clutter power is given by

$$\hat{\tau} = \left(\frac{1}{\beta_1} \sum_{k=1}^{\alpha_1} |n_k|^2 \right)^{-1}, \quad (10)$$

where n_k is a complex random number, and its statistics are a complex Gaussian distribution with zero mean and unit variance.
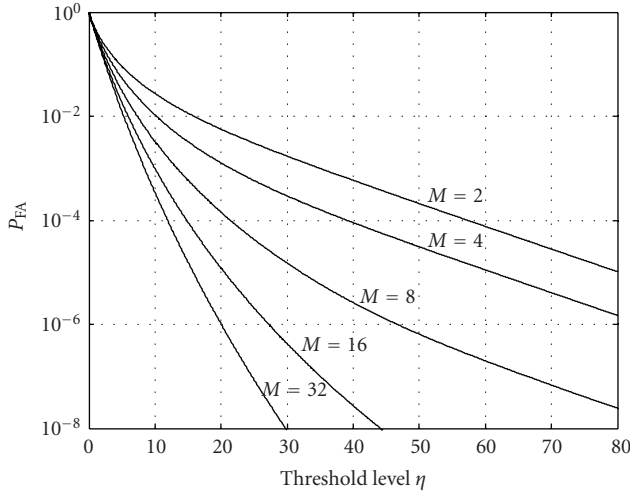
FIGURE 2: Example of threshold level in proposed CFAR.

2.2.2. Hyperparameters. The hyperparameters are not known a priori. Thus, a noninformative prior [17, 19, 20] that is one of the approaches to obtaining the hyperparameters is considered in this study. By using the noninformative prior, a prior distribution is regarded as uniform. Thus, $\alpha_0 \to 0$ and $\beta_0 \to \infty$ should be used. However, the parameters are set to $\alpha_0 = 1$ and $\beta_0 = 0$. For the former value, because the estimated local clutter power in the CUT is given by (10) and α_1 as the summation index, it must be a natural number. From (7), α_0 is also a natural number. Therefore, $\alpha_0 = 1$, that is, the smallest natural number, is used. Meanwhile for the latter value $\beta_0 = 0$ is used (though this should be a large number) because a false alarm rate is to be derived analytically. If β_0 is not a zero, the distribution of β_1 is not a Gamma distribution (i.e., the distribution of Y_1 in (A.5) is not the Chi-square distribution in the appendix). Therefore, it is extremely difficult to derive the false alarm rate. The discussion of detection performance dependence on the parameters is in Section 3.1.

2.2.3. Local Clutter Estimation. In (3), X is assumed as the clutter. However, this assumption cannot be accepted in actual detection scenarios since whether X includes the target signal or not is unknown. Therefore, we propose replacing X in (3) with the estimated clutter from the data in the reference cells. The Bayesian theory is also applied for the estimation. The estimated clutter denoted as $\hat{C}$ is given as mean of the Bayesian predictive density function (MBPDF). In the MBPDF, $\hat{C}$ is represented by

$$\hat{C} = \int_0^\infty C P^*(C \mid D) dC, \tag{11}$$

where $P^*(C \mid D)$ is the predictive density [17, 19, 21, 22]. This is defined by

$$P^*(C \mid D) = \int_0^\infty p(C \mid \tau) p(\tau \mid D) d\tau, \tag{12}$$

where $p(C \mid \tau) = 1/\tau e^{-C/\tau}$ and $p(\tau \mid D)$ is the posterior distribution, that is, $p(\tau \mid D) \propto L(\tau \mid D) p(\tau)$. The likelihood function is given by

$$L(\tau \mid D) = \prod_{m=1}^M p(X_m \mid \tau). \tag{13}$$

Since the prior distribution is also supposed as the inverse Gamma distribution with the hyperparameters as a_0 and b_0, that is, $p(\tau) = IG(\tau; a_0, b_0)$; the posterior distribution is thus the inverse Gamma distribution, $p(\tau|D) = IG(\tau; a_1, b_1)$ with the hyperparameters as

$$a_1 = M + a_0,$$

$$b_1 = \sum_{m=1}^M X_m + b_0. \tag{14}$$

Substitute $p(C \mid \tau)$ and $p(\tau \mid D)$ into (12), then

$$P^*(C \mid D) \propto \frac{\Gamma(a_1 + 1)}{(X + b_1)^{a_1+1}}, \tag{15}$$

where "$\propto$" signifies "proportional to." Therefore, $\hat{C}$ is given by

$$\hat{C} = A \cdot \Gamma(a_1 - 1) b_1^{-a_1+1}, \tag{16}$$

where A is a constant. Since the hyperparameters are not known, the noninformative prior as described in Section 2.2.2 is applied. Thus, $a_0 = 0.1$ and $b_0 = 10$ are given. Contrary to hyperparameters α_0 and β_0 in Section 2.2.2, these values of a_0 and b_0 do not affect a false alarm derivation. With these values, the prior distribution, that is, the inverse Gamma distribution, is approximated as uniform. In the local clutter power estimation in Section 2.2.1, the posterior distribution of the power is then estimated with $\hat{C}$ instead of X, that is, X is replaced with $\hat{C}$.

2.2.4. False Alarm Rate and Probability of Detection. The expressions of the false alarm rate P_{FA} and the probability of detection P_D are described in the appendix; P_{FA} and P_D are given by (A.11) and (A.13), respectively. Note that P_{FA} is independent of the statistical parameters of the clutter. Therefore the proposed technique offers CFAR capability with respect to the clutter. Also note that P_{FA} and P_D include integration as the confluent hypergeometric function of the second kind [23] and the calculation of the threshold is slightly difficult. In Figure 2, we show examples of P_{FA} versus η for various M.

Figure 3 shows a block diagram of the proposed detection technique. In Figure 3(a), first, the sum of X_m is calculated from the reference cells, and then the clutter in the CUT is estimated by the MBPDF (the detailed process is shown in Figure 3(b)). Using the estimated clutter and the sum of X_m, the local clutter power distribution in the CUT is estimated by the Bayesian theory and the estimated power $\hat{\tau}$ is produced numerically by the Gaussian random number generator (the detail is shown in Figure 3(c)). Then the data in the CUT X
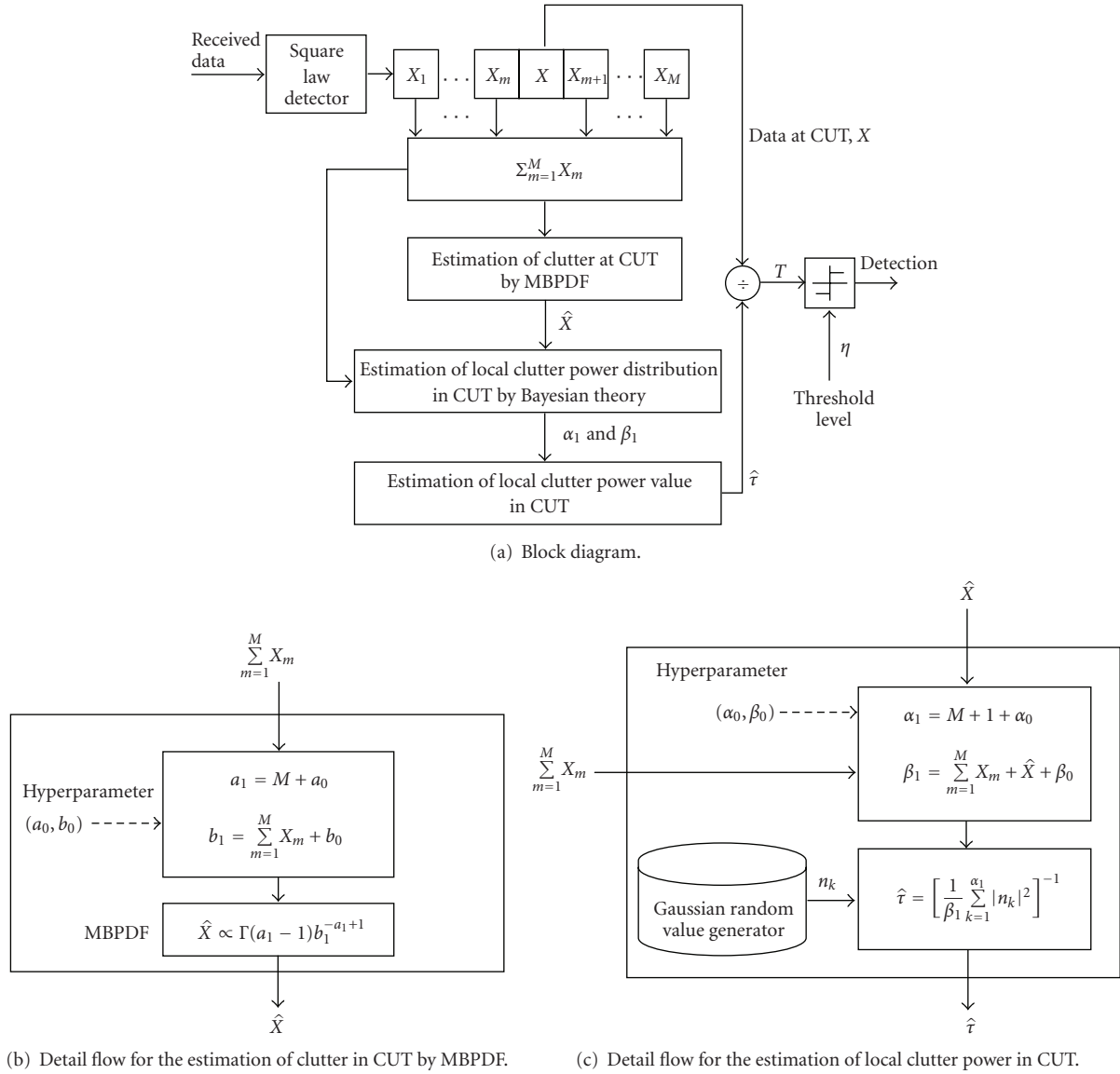
(a) Block diagram.

(b) Detail flow for the estimation of clutter in CUT by MBPDF.

(c) Detail flow for the estimation of local clutter power in CUT.

FIGURE 3: Block diagram of proposed detection technique.

is divided by $\hat{\tau}$. Finally, the test statistic T is compared with the threshold level η to determine whether the target signal is present.

3. Performance Analysis

In this section, the detection performance is numerically investigated by Monte Carlo simulations. To determine the validity of the proposed technique when applying the inverse Gamma prior distribution of the local clutter power, the sea clutter in the simulation is given as the K distribution. Thus, the local clutter power is Gamma distributed (not inverse Gamma). The K distribution is a function of the shape parameter ν and the scale parameter θ. Generally, the distributions with a small and large ν are far from and close to the exponential distribution, respectively. The mean of the local clutter power is represented by $\nu\theta$. The local clutter

power is spatially correlated in range and its autocorrelation function is defined as [24]

$$\mathrm{ACF}(i) = \frac{E\{\tau_m \tau_{m+i}\}}{E\{\tau_{m^2}\}}, \qquad (17)$$

where $E\{\cdot\}$ is an expectation, i is the shift of range cell, and τ_m is the local clutter power in the range cell m. In this simulation, the autocorrelation function is given by [25]

$$\mathrm{ACF}(i) = \rho^i, \qquad (18)$$

where ρ is the correlation coefficient. The shift at which the $\mathrm{ACF}(i)$ is equal to $1/e$ is defined as the correlation range cell, denoted as i_C. The i_C is a measure of the rate of the local clutter power decorrelation; if two clutter cells are separated by a distance greater than i_C, then their local clutter powers may be considered to be statistically independent.

(a) Clutter and its texture
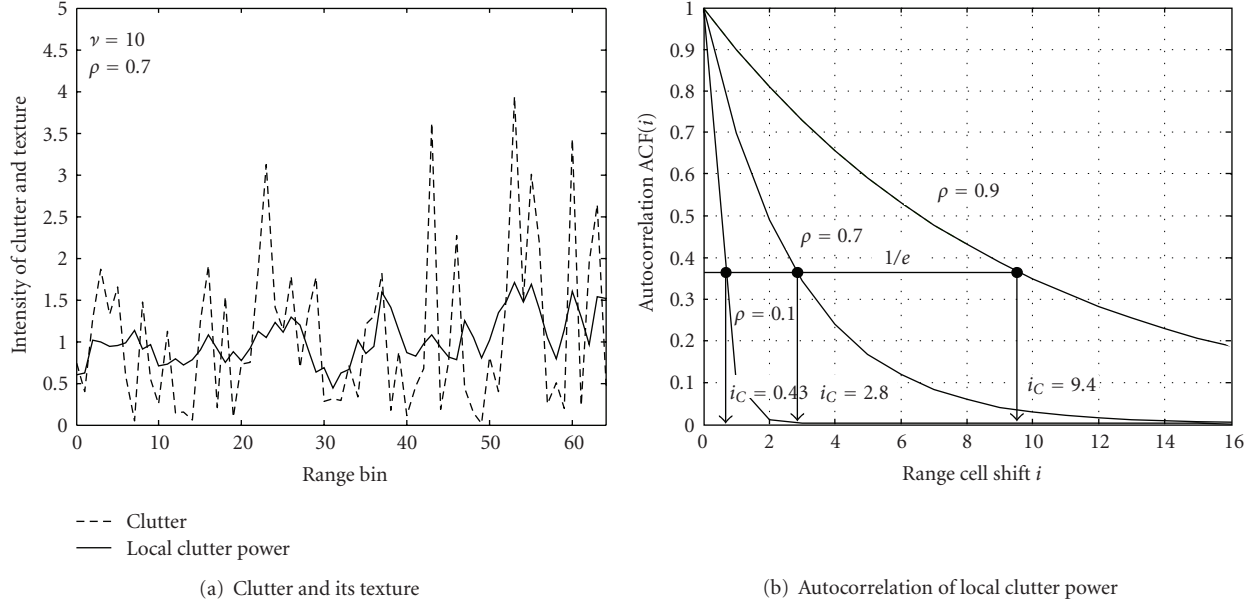

(b) Autocorrelation of local clutter power

FIGURE 4: Example of simulated clutter and the autocorrelation function of local clutter power.

Figure 4 shows an example of the simulated clutter and the autocorrelation function of the local clutter power. In Figure 4(a), the spatial clutter power fluctuation and strong clutter intensities (like as a spiky clutter) observed in range cells of 22, 44, and 53 are simulated. In Figure 4(b), the autocorrelation function with $\rho = 0.1$, 0.7, and 0.9 is shown and their correlation range cells are expressed by $i_C = -1/\ln\rho$, that is, $i_C = 0.43$, 2.8, and 9.4, respectively. The signal to clutter ratio denoted by SCR is defined as SCR $= \tau_T/\nu\theta$, where τ_T is the mean of the signal intensity (i.e., the signal power). The threshold level is set to $P_{FA} = 10^{-4}$, and a total of 1×10^6 independent Monte Carlo runs were performed.

3.1. Performance Characteristics. The hyperparameters, α_0 and β_0 in (6), should be given in accordance with the noninformative prior; $\alpha_0 \to 0$ and $\beta_0 \to \infty$. However $\alpha_0 = 1$ and $\beta_0 = 0$ are given as described in Section 2.2.2. Particularly, the value of β_0 is in conflict with the noninformative prior. Therefore, the effect of α_0 and β_0 on the probability of detection P_D should be investigated. Figure 5 shows the simulation results for the investigation, where $M = 2$ and $\nu = \infty$ (i.e., the exponential distributed clutter; homogeneous clutter), and the results of an ideal detector are also shown. The ideal detector is defined as the CA-CFAR with known local clutter power in the CUT; it provides the maximum P_D. In Figure 5(a), where $\beta_0 = 0$, it is found that P_D for each α_0 is almost the same and is independent of α_0. In Figure 5(b), where $\alpha_0 = 1$, it is shown that P_D is improved by increasing β_0. From these results, it is expected that the value of a larger β_0 gives a higher P_D. However, in this study, $\beta_0 = 0$ is chosen because of the analytical P_{FA} derivation.

Figure 6 shows the effect of the number of reference cells M on P_D, where $\nu = \infty$ and $\nu = 0.5$ (heterogeneous clutter) are given. Figure 6(a) shows the result of the clutter with

$\nu = \infty$. It can be seen that P_D generally increases with M and is close to the P_D curve for the ideal detector. From the P_D for the ideal detector, the CFAR loss [18] at $M = 2$ and $P_D = 0.5$ is about 9 dB. Note that the loss of the CA-CFAR is more than 10 dB at the same M and P_D [2]. The CFAR loss of the proposed technique is found to be small. The accuracy of the estimated local clutter power is superior to the CA-CFAR and the P_D is higher. Figure 6(b) shows the result for clutter with $\nu = 0.5$ and $\rho = 0$. The clutter distribution deviates considerably from the exponential and the condition of the local clutter power estimation is severe since the local clutter power is not correlated. It can also be seen that P_D increases with M. From P_D for the ideal detector, the CFAR loss at $M = 2$ and $P_D = 0.5$ is about 20 dB. Compared with the homogeneous clutter shown in Figure 6(a), P_D decreases and the CFAR loss increases.

Figure 7 shows the effect of ν on P_D, where $M = 2$, and $\rho = 0$ and 0.9. In Figure 7(a) for clutter with $\rho = 0$, P_D increases with ν. It is worth remembering that the K distribution with a large ν is approximately the exponential (homogeneous) distribution. Thus, the proposed technique for homogeneous clutter provides higher P_D than for the heterogeneous one. This phenomenon was also observed in the CA-CFAR [8]. Meanwhile in Figure 7(b), for clutter with $\rho = 0.9$, P_D is almost the same for each value of ν and is close to that for $\nu = 10$ in Figure 7(a). This is because the correlation length ($i_C = 9.4$ in Figure 4(b)) encompasses the reference cells for $M = 2$; thus, the local clutter power in the reference cells can be regarded as the same as that in the CUT.

Figure 8 shows the effect of the local clutter power correlation ρ on P_D, where $\nu = 0.5$ and $M = 2$ and 16. In Figure 8(a) for $M = 2$ (i.e., a small number of reference cells), P_D increases with ρ. In the clutter with large ρ and small M, as seen in Figure 7(b) for $\rho = 0.9$, the local clutter power spatial fluctuation drops and the local clutter power

(a) Effect of α_0; $\beta_0 = 0$

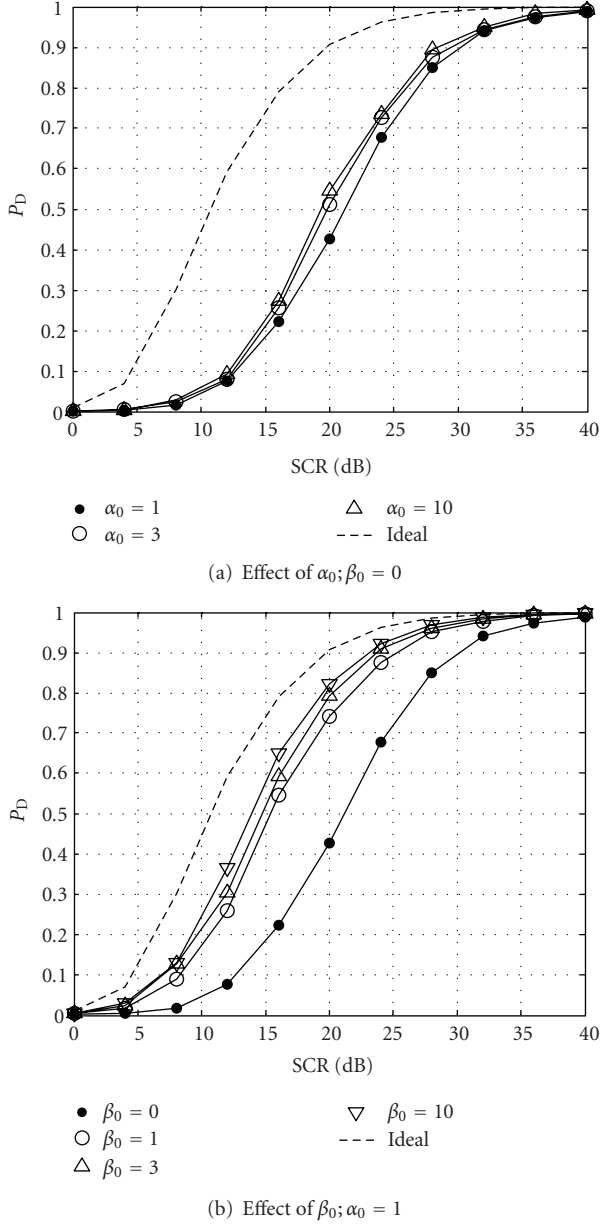(b) Effect of β_0; $\alpha_0 = 1$

FIGURE 5: Effect of hyperparameters on P_D; $M = 2$, $\nu = \infty$ (exponential distribution).

in the reference cell can be regarded as that in the CUT. Therefore, the accuracy of the local clutter power estimation is enhanced and P_D becomes high. In Figure 8(b) for $M = 16$ (i.e., a large number of cells), the P_D for $\rho = 0.9$ is the highest. Meanwhile, P_D, except for $\rho = 0.9$, is almost the same because the values of i_C for the clutter with $\rho = 0.1$ to 0.7, which are $i_C = 0.43$ to 2.8, respectively, are considerably smaller than the number of reference cells. The local clutter power varies in the reference cells and the accuracy of the local clutter power estimation is then degraded.

Here, we consider guard cells effect on the performance. The spatial correlation between the local clutter power in the CUT and reference cells decreases with the increase of the

number of guard cells. From the results of the effect of ρ as shown in Figure 8, therefore, the probability might depend on guard cells. For example, for a small number of reference cells, P_D decreases with the increase of number of guard cells as observed in Figure 8(a).

3.2. Performance Comparison. It may be interesting to make a comparison with conventional CFAR. Here, the CFAR techniques with the following local clutter power estimation methods of ML (i.e., conventional CA-CFAR), MAP, and MMSE (Bayes risk minimization) are considered.

The ML estimator is a simple method and no prior information of the local clutter power is needed. The local clutter power is estimated by

$$\hat{\tau}_{\mathrm{ML}} = \arg \max_{\tau} L(\tau \mid D) = \overline{X}_m, \qquad (19)$$

where $\overline{X}_m = (1/M) \sum_{m=1}^{M} X_m$ and X_m is the exponential distribution conditioned on τ, defined by the right side in (5). The likelihood function $L(\tau \mid D)$ in (19) is

$$L(\tau \mid D) = \prod_{m=1}^{M} p(X_m \mid D). \qquad (20)$$

In the ML, the local clutter power is given by the mean of the reference data. When this estimator is used, the resulting detection structure is given by the well known CA-CFAR.

The MAP estimator depends on the details of the local clutter power distribution $p(\tau)$. Since the K distributed clutter is used in this simulation, the statistics of the local clutter power are then given as a Gamma distribution
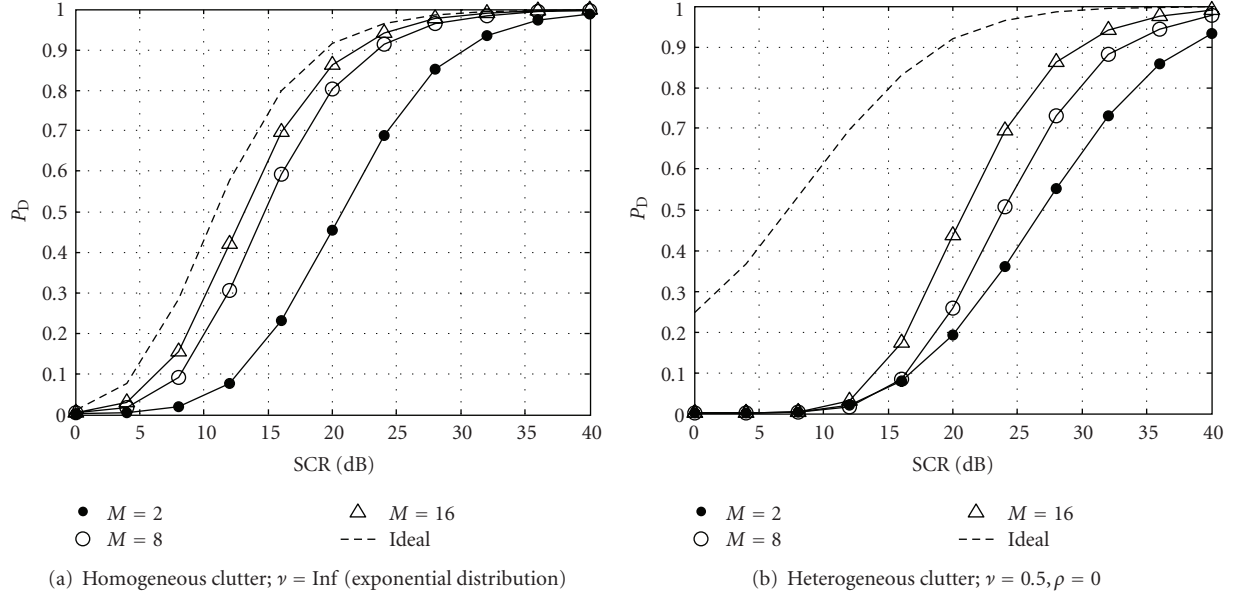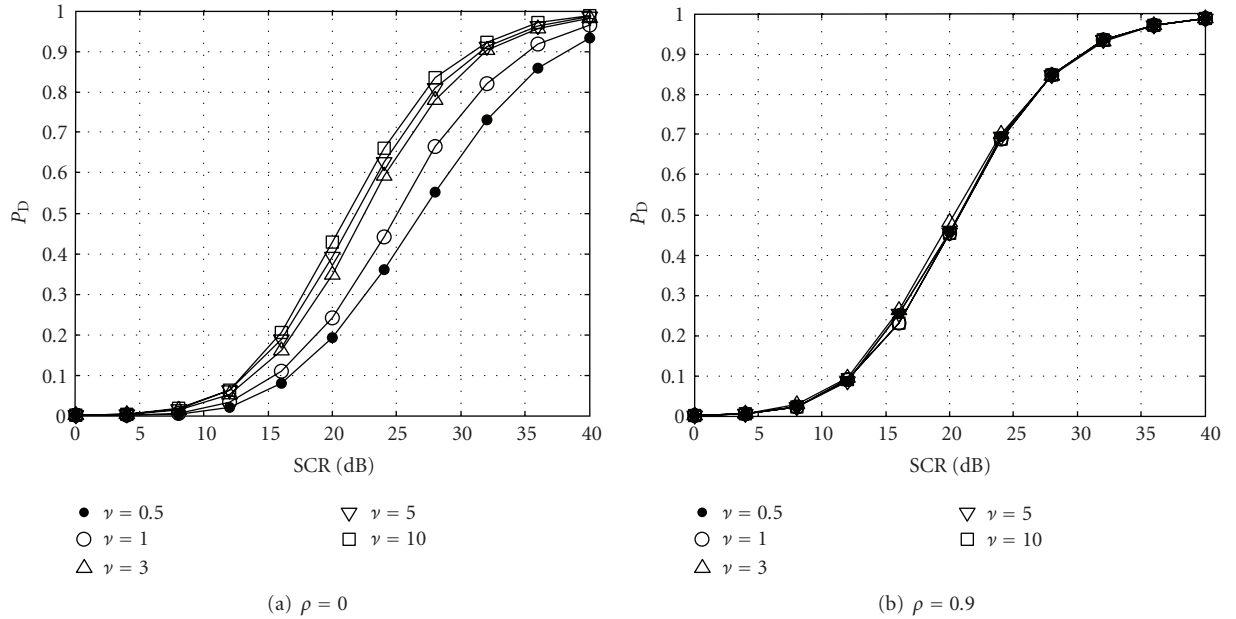
$$p(\tau) = \frac{1}{\theta_M \Gamma(\nu_M)} \tau^{\nu_M - 1} e^{-\tau/\theta_M}, \qquad (21)$$

where θ_M and ν_M are the scale and shape parameters. The statistics of the speckle are the exponential conditioned on τ, that is, the local clutter power. The MAP estimator is found by maximizing a posterior distribution $p(\tau \mid D) \propto L(\tau \mid D)p(\tau)$. From the likelihood function in (20) and the prior distribution in (21), the result is

$$\begin{aligned} \hat{\tau}_{\mathrm{MAP}} &= \arg \max_{\tau} p(\tau \mid D) \\ &= \arg \max_{\tau} L(\tau \mid D)p(\tau) \\ &= -\frac{1}{2}(M - \nu_M + 1)\theta_M \\ &\quad + \sqrt{\frac{1}{4}(M - \nu_M + 1)^2 \theta_M{}^2 + M\overline{X}_m \theta_M}. \end{aligned} \qquad (22)$$

The MMSE estimator also depends on the details of the local clutter power distribution $p(\tau)$, given as a Gamma distribution. The estimated value by the MMSE is represented as [26]

$$\begin{aligned} \hat{\tau}_{\mathrm{MMSE}} &= \int_0^{\infty} \tau p(\tau \mid D) d\tau \\ &= \int_0^{\infty} \tau \frac{L(\tau \mid D)p(\tau)}{\int_0^{\infty} L(\tau \mid D)p(\tau)d\tau} d\tau, \end{aligned} \qquad (23)$$

(a) Homogeneous clutter; $\nu = \text{Inf}$ (exponential distribution)

(b) Heterogeneous clutter; $\nu = 0.5, \rho = 0$

FIGURE 6: Effect of M on P_D.

(a) $\rho = 0$

(b) $\rho = 0.9$

FIGURE 7: Effect of ν on P_D; $M = 2$.

where $p(\tau \mid D)$ is the posterior distribution. Substituting the likelihood in (20) and the prior in (21) into (23), the estimated local clutter power is given by

$\hat{\tau}_{\text{MMSE}}$

$$= \sqrt{\theta_M M \overline{X}_m} \cdot K_{M-\nu_M-1}\left(\sqrt{\frac{4M\overline{X}_m}{\theta_M}}\right) \bigg/ K_{M-\nu_M}\left(\sqrt{\frac{4M\overline{X}_m}{\theta_M}}\right),$$

(24)

where $K_p(x)$ is the modified Bessel function of second kind of order p.

In (22) and (24), the estimated local clutter powers, $\hat{\tau}_{\text{MAP}}$ and $\hat{\tau}_{\text{MMSE}}$, are the function of the parameters, θ_M and ν_M. Thus, knowledge of these parameters is needed a priori. If the parameters are unknown, they are estimated. Thus, the probability of detection also depends on the estimation technique. To remove the estimation effect on the probability of detection, the proposed technique is compared with conventional CFAR schemes with known parameters. Thus, in this comparison, these conventional schemes are not meant as realizable detectors. However, if the proposed technique is superior to the conventional one when using
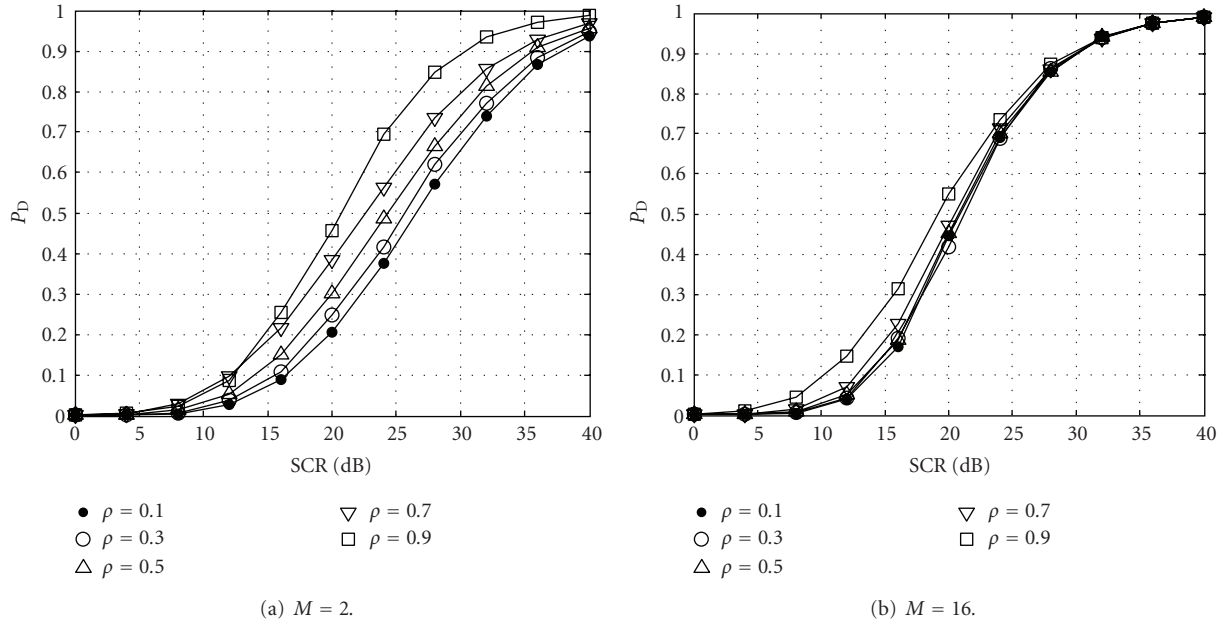
(a) $M = 2$.

(b) $M = 16$.

FIGURE 8: Effect of ρ on P_D; $\nu = 0.5$.

known parameters, the probability of detection is higher than that in the conventional with estimated parameters. This is because, when using estimated parameters, the conventional method provides lower probability than with known parameters due to errors arising from the estimation. Therefore, in this comparison, these parameters are assumed as completely known and are set with the same values for the simulated sea clutter, that is, $\theta_M = \theta$ and $\nu_M = \nu$.

In the performance comparison, the K distributed clutter with $\nu = 0.5$, and the two with local clutter power spatial correlation, $\rho = 0.1$ and 0.9, are used. Figure 9(a) compares the proposed detection method with the results of ML, MAP and MMSE estimator, where $M = 2$ and the clutter with $\rho = 0.1$. This provides a severe situation for the local clutter power estimation since the number of reference cells is small and the local clutter power fluctuates extremely. The proposed technique significantly outperforms the conventional ones. For example, at $P_D = 0.5$, the SCR enhancement is 13 dB compared with MMSE. Figure 9(b) shows the performance comparison under $M = 2$ and $\rho = 0.9$. This also provides the severe conditions; however, the local clutter power fluctuation is more moderate than in Figure 9(a). Again, the proposed technique outperforms the conventional ones. Figure 9(c) shows the performance comparison under $M = 16$ and $\rho = 0.1$. In this condition, the number of reference cells M is considerably large relative to the correlation range cell ($i_C = 0.43$). The performance is almost the same, and P_D enhancement by the proposed should not be expected. Figure 9(d) shows the comparison under $M = 16$ and $\rho = 0.9$. Similar to Figure 9(c), P_D remains almost the same.

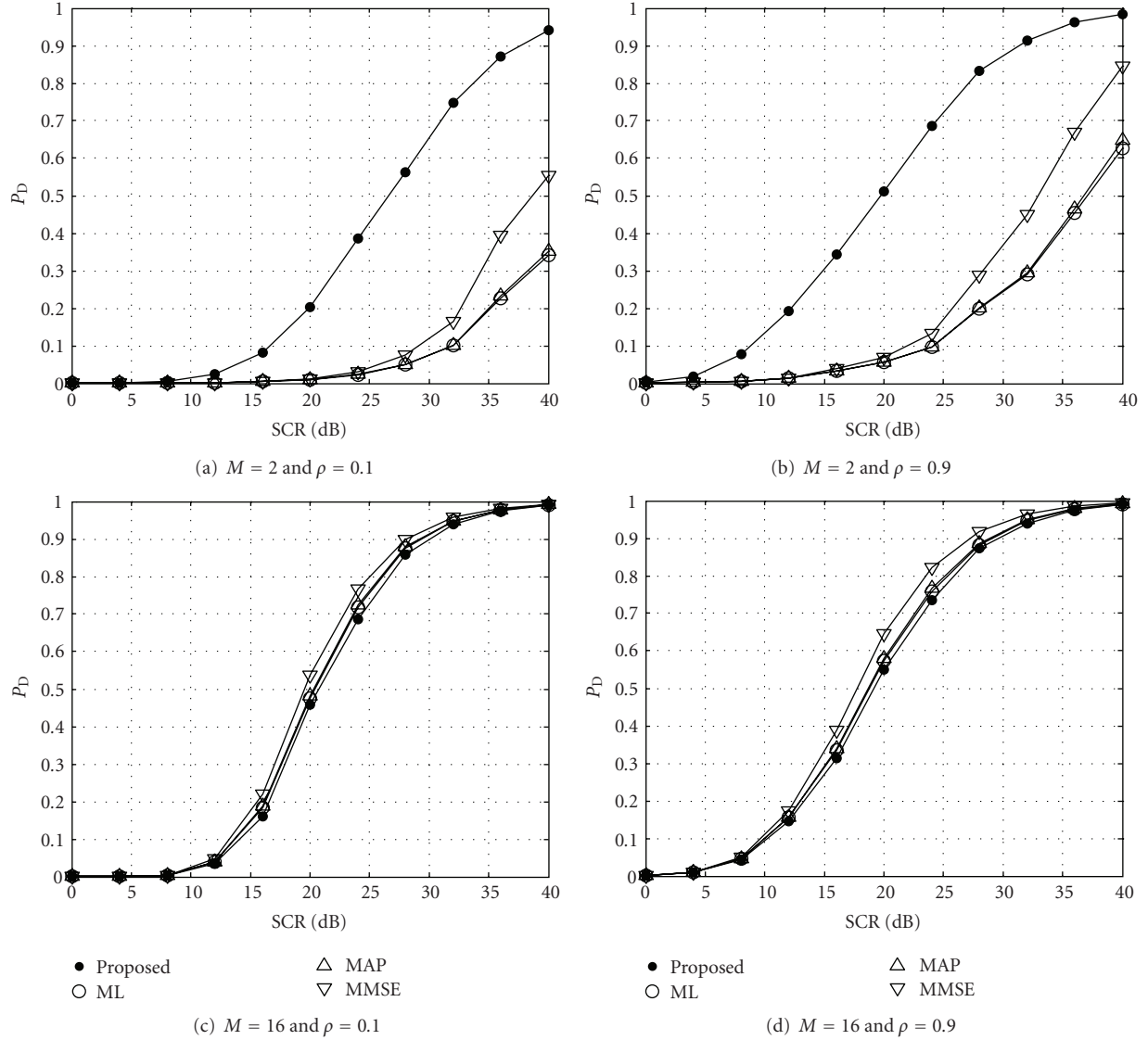These results show that the proposed technique is superior to CFAR with ML, MAP, and MMSE estimator, especially when the number of reference cells is small and the local clutter power spatial correlation is weak.

4. Conclusions

In this paper, a CFAR detection technique in sea clutter for noncoherent radar systems was introduced, where heterogeneous sea clutter is considered. The technique mainly applies the Bayesian theory for adaptive estimation of the local clutter power in the CUT. The technique achieves detection with no prior clutter information and has the CFAR property with respect to the clutter. We investigated the detection performance through Monte Carlo simulations where K distributed sea clutter with spatially correlated local clutter power was used. The following conclusions can be drawn from the simulation results.

(1) The detection performance of the proposed technique depends on the number of reference cells, the sea clutter distribution, and the spatial correlation of the local clutter power. The probability of detection increases with the number of cells, the shape parameter of the sea clutter, and the correlation.

(2) The proposed technique is found to be very useful compared with the conventional CFAR detector in which the shape and the scale parameters are known a priori, especially when the number of reference cells is small and the spatial correlation of the local clutter power is weak.

In a future study, we will investigate the detection performance enhancement in a large number of reference cells, analyze performance with the measured sea clutter data, and further investigate the implementation of the proposed

(a) $M = 2$ and $\rho = 0.1$

(b) $M = 2$ and $\rho = 0.9$

(c) $M = 16$ and $\rho = 0.1$

- Proposed   △ MAP
○ ML   ▽ MMSE

(d) $M = 16$ and $\rho = 0.9$

- Proposed   △ MAP
○ ML   ▽ MMSE

FIGURE 9: Performance comparison; $\nu = 0.5$ $(2/2, 1/2)$.

technique into a collision avoidance radar system for ships or pleasure boat safety navigation.

Appendix

We derive the false alarm rate P_{FA}. X is thus the clutter. Here, we slightly modify (2), where both the numerator and denominator are divided by the true local clutter power, τ,

$$T = \frac{X/\tau}{\widehat{\tau}/\tau}. \tag{A.1}$$

When the CUT does not include the target signal, the probability density function (pdf) of X is the exponential distribution with τ of the mean. Thus the pdf of the numerator in (A.1) is the exponential with unit variance. Next we consider the pdf of the denominator. Since the pdf of $\widehat{\tau}$ is expressed as the inverse Gamma distribution,

as expressed in (9), $\widehat{\tau}$ belonging to this distribution can be expressed as

$$\widehat{\tau} \sim \left(\sum_{m=1}^{\alpha_1} |y_m|^2 \right)^{-1}, \tag{A.2}$$

where α_1 is the order parameter given in (7), and the distribution of y_m is the noncorrelated complex Gaussian distribution with zero mean and β_1 of the variance. Here, (A.2) is further modified as

$$\widehat{\tau} \sim \beta_1 \left(\sum_{m=1}^{\alpha_1} |n_m|^2 \right)^{-1}, \tag{A.3}$$

where the pdf of n_m is the noncorrelated complex Gaussian distribution with zero mean and unit variance. Substituting

(8) into (A.3), the distribution of the numerator $\hat{\tau}/\tau$ is given by

$$
\frac{\hat{\tau}}{\tau} \sim \frac{1}{\tau} \left\{ \sum_{m=1}^{M} X_m + X + \beta_0 \right\} \left(\sum_{m=1}^{\alpha_1} |n_m|^2 \right)^{-1} = \frac{Y_1}{Y_2}, \quad \text{(A.4)}
$$

where

$$
Y_1 = \frac{1}{\tau} \left\{ \sum_{m=1}^{M} X_m + X + \beta_0 \right\}, \qquad Y_2 = \sum_{m=1}^{\alpha_1} |n_m|^2. \quad \text{(A.5)}
$$

Since $\beta_0 = 0$, and X_m and X are the clutter, the distribution of Y_1 is the Chi-square distribution with $M + 1$ degrees of freedom, denoted by χ_{M+1}^2. Similarly, the distribution of Y_2 is given by $\chi_{\alpha_1}^2$. Here, Y_1/Y_2 is slightly modified as

$$
\frac{Y_1}{Y_2} = \frac{Y_1/(M+1)}{Y_2/\alpha_1} \cdot \frac{M+1}{\alpha_1}
$$
$$
= z_0 \times \frac{M+1}{\alpha_1}, \quad \text{(A.6)}
$$

where

$$
z_0 \equiv \frac{Y_1/(M+1)}{Y_2/\alpha_1}. \quad \text{(A.7)}
$$

Since the pdf of z_0 is the F distribution [27], the pdf of $z \equiv Y_1/Y_2$ (i.e., the denominator in (A.1)) is given by

$$
p(z)dz = \frac{\Gamma(M+1+\alpha_1)}{\Gamma(M+1)\Gamma(\alpha_1)} \cdot \frac{z^M}{(1+z)^{M+1+\alpha_1}} dz, \quad \text{(A.8)}
$$

where $\Gamma(\cdot)$ is the Gamma function. Therefore, the distribution of T is represented by

$$
p(T)dT = (M+1) \frac{\Gamma(M+1+\alpha_1)}{\Gamma(\alpha_1)} \cdot U(M+2; 2-\alpha_1; T)dT, \quad \text{(A.9)}
$$

where $U(a; b; x)$ is the confluent hypergeometric function of the second kind [23], expressed by

$$
U(a; b; x) = \frac{1}{\Gamma(a)} \int_0^\infty \frac{g^{a-1}}{(1+g)^{a+1-b}} e^{-xg} dg. \quad \text{(A.10)}
$$

Finally, P_{FA} as a function of η is given by

$$
P_{\text{FA}}(\eta) = \int_\eta^\infty p(T)dT
$$
$$
= \frac{\Gamma(M+1+\alpha_1)}{\Gamma(\alpha_1)} \cdot U(M+1; 1-\alpha_1; \eta). \quad \text{(A.11)}
$$

From (A.11), P_{FA} is not a function of the statistical parameter τ of the clutter.

Next, we derive the probability of detection, P_D. Since the signal is assumed as the Swerling I model described in Section 2.1, the random variable of the numerator in (A.1), that is, X/τ, is expressed as the exponential distribution with $1 + \tau_T/\tau$ of the mean, where τ_T is the mean of the signal intensity (i.e., the signal power). On the other hand, the distribution of denominator in (A.1) is also given by (A.8). Similar to the derivation of P_{FA}, the distribution of T is thus

$$
p(T)dT = \frac{M+1}{1+\tau_T/\tau} \cdot \frac{\Gamma(M+1+\alpha_1)}{\Gamma(\alpha_1)}
$$
$$
\cdot U\left(M+2; 2-\alpha_1; \frac{T}{1+\tau_T/\tau}\right)dT. \quad \text{(A.12)}
$$

Therefore, P_D as a function of η, is given by

$$
P_D(\eta) = \int_0^\eta p(T)dT
$$
$$
= \frac{\Gamma(M+1+\alpha_1)\Gamma(M+1)}{\Gamma(\alpha_1)} \cdot U\left(M+1; 1-\alpha_1; \frac{\eta}{1+\tau_T/\tau}\right). \quad \text{(A.13)}
$$

In (A.13), it is found that P_D is a function of M, α_1, and τ_T/τ.

References

[1] E. Jakeman and P. N. Pusey, "A model for non-Gaussian sea echo," *IEEE Transactions on Antennas and Propagation*, vol. 24, no. 6, pp. 806–818, 1976.

[2] V. G. Hansen and H. R. Ward, "Detection performance of the cell averaging LOG/CFAR receiver," *IEEE Transactions on Aerospace and Electronic Systems*, vol. 8, no. 5, pp. 648–652, 1972.

[3] M. Sekine, T. Musha, Y. Tomita, and T. Irabu, "Suppression of Weibull distributed clutters using a cell-averaging log CFAR receiver," *IEEE Transactions on Aerospace and Electronic Systems*, vol. 14, no. 5, pp. 823–826, 1978.

[4] V. Anastassopoulos, G. A. Lampropoulos, A. Drosopoulos, and M. Key, "High resolution radar clutter statistics," *IEEE Transactions on Aerospace and Electronic Systems*, vol. 35, no. 1, pp. 43–60, 1999.

[5] S. Haykin, C. Krasnor, T. J. Nohara, B. W. Currie, and D. Hamburger, "A coherent dual-polarized radar for studying the ocean environment," *IEEE Transactions on Geoscience and Remote Sensing*, vol. 29, no. 1, pp. 189–191, 1991.

[6] F. Gini, M. V. Greco, M. Diani, and L. Verrazzani, "Performance analysis of two adaptive radar detectors against non-Gaussian real sea clutter data," *IEEE Transactions on Aerospace and Electronic Systems*, vol. 36, no. 4, pp. 1429–1439, 2000.

[7] S. Watts, "Radar detection prediction in K-distributed sea clutter and thermal noise," *IEEE Transactions on Aerospace and Electronic Systems*, vol. 23, no. 1, pp. 40–45, 1987.

[8] S. Watts, "The performance of cell-averaging CFAR systems in sea clutter," in *Proceedings of the IEEE National Radar Conference*, pp. 398–403, May 2000.

[9] S. Watts and K. D. Ward, "Spatial correlation in K-distributed sea clutter," *IEE Proceedings F*, vol. 134, no. 6, pp. 526–532, 1987.

[10] K. J. Sangston, F. Gini, M. V. Greco, and A. Farina, "Structures for radar detection in compound Gaussian clutter," *IEEE Transactions on Aerospace and Electronic Systems*, vol. 35, no. 2, pp. 445–458, 1999.

[11] R. C. Colgin, "Description and analysis of a Bayesian CFAR, radar signal processor in a nonhomogeneous clutter background," in *Proceedings of the IEEE National Radar Conference*, pp. 3–8, Dallas, Tex, USA, May 1998.

[12] R. J. A. Tough, K. D. Ward, and P. W. Shepherd, "The modelling and exploitation of spatial correlation in spiky sea clutter," in *Proceedings of the 2nd European Radar Conference (EURAD '05)*, pp. 5–8, Paris, France, October 2005.

[13] M. Weiss, "Analysis of some modified cell-averaging CFAR processors in multiple target situations," *IEEE Transactions on Aerospace and Electronic Systems*, vol. 18, no. 1, pp. 102–114, 1982.

[14] E. Jay, J. P. Ovarlez, D. Declercq, and P. Duvaut, "BORD: Bayesian optimum radar detector," *Signal Processing*, vol. 83, no. 6, pp. 1151–1162, 2003.

[15] K. J. Sangston and K. R. Gerlach, "Coherent detection of radar targets in a non-Gaussian background," *IEEE Transactions on Aerospace and Electronic Systems*, vol. 30, no. 2, pp. 330–340, 1994.

[16] F. Gini, G. B. Giannakis, M. Greco, and G. T. Zhou, "Time-averaged subspace methods for radar clutter texture retrieval," *IEEE Transactions on Signal Processing*, vol. 49, no. 9, pp. 1886–1898, 2001.

[17] D. Gamerman, *Markov Chain Monte Carlo: Stochastic Simulation for Bayesian Inference*, Chapman & Hall/CRC, Boca Raton, Fla, USA, 2002.

[18] M. I. Skolnik, *Radar Handbook*, McGraw-Hill, Boston, Mass, USA, 2nd edition, 1990.

[19] H. Watanabe, *Introduction to Bayesian Statistics*, Fukumura Press, 2003.

[20] N. Ueda, "Bayesian learning. [II]: introduction to Bayesian learning," *Journal of the IEICE*, vol. 85, no. 6, pp. 421–426, 2002.

[21] C.-M. Cho and P. M. Djurić, "Detection and estimation of DOA's of signals via Bayesian predictive densities," *IEEE Transactions on Signal Processing*, vol. 42, no. 11, pp. 3051–3060, 1994.

[22] P. M. Djurić and S. M. Kay, "Predictive probability as a criterion for model selection," in *Proceedings of the IEEE International Conference on Acoustics, Speech, and Signal Processing (ICASSP '90)*, vol. 5, pp. 2415–2418, 1990.

[23] L. C. Andrews, *Special Functions of Mathematics for Engineers*, Oxford University Press, Oxford, UK, 2nd edition, 1998.

[24] F. T. Ulaby, R. K. Moore, and A. K. Fung, *Microwave Remote Sensing: Active and Passive*, Artech House, London, UK, 1986.

[25] F. F.Gini and M.V. Greco, "Suboptimum approach to adaptive coherent radar detection in compound-Gaussian clutter," *IEEE Transactions on Aerospace and Electronic Systems*, vol. 35, no. 3, pp. 1095–1104, 1999.

[26] T. Katayama, *Applied Kalman Filtering*, Asakura Shoten, 2005.

[27] L. L. Scharf, *Statistical Signal Processing: Detection, Estimation, and Time Series Analysis*, Addison-Wesley, New York, NY, USA, 1991.